PAPER

# BER Performance Analysis of MC-CDMA with Overlap-FDE

**Hiromichi TOMEBA**[†a)], **Kazuaki TAKEDA**[†], ***Student Members***, ***and*** **Fumiyuki ADACHI**[†], ***Fellow***

**SUMMARY** Recently, multi-carrier code division multiple access (MC-CDMA) has been attracting much attention as a broadband wireless access technique for the next generation mobile communication systems. Frequency-domain equalization (FDE) based on the minimum mean square error (MMSE) criterion can take advantage of the channel frequency-selectivity and improve the average bit error rate (BER) performance due to frequency-diversity gain. The conventional FDE requires the insertion of the guard interval (GI) to avoid the inter-block interference (IBI), resulting in the transmission efficiency loss. In this paper, an overlap FDE technique, which requires no GI insertion, is presented for MC-CDMA transmission. An expression for the conditional BER is derived for the given set of channel gains. The average BER performance in a frequency-selective Rayleigh fading channel is evaluated by Monte-Carlo numerical computation method using the derived conditional BER and is confirmed by computer simulation of the signal transmission.

***key words:*** *frequency-selective fading channel, overlap FDE, MC-CDMA*

## 1. Introduction

Broadband data services are demanded in the next generation mobile communication systems. However, the broadband mobile channel is composed of many propagation paths with different time delays, producing severe frequency-selective fading channel, and the transmission performance degrades due to severe inter-symbol interference (ISI) [1], [2]. Recently, multi-carrier code division multiple access (MC-CDMA), which uses a number of lower-rate orthogonal subcarriers to reduce the ISI resulting from frequency-selective channel, has been attracting much attention [3]–[5]. A good bit error rate (BER) performance can be achieved by using frequency-domain equalization (FDE) based on the minimum mean square error (MMSE) criterion [5]. MMSE-FDE can also be applied to the single-carrier transmission, e.g., direct-sequence CDMA (DS-CDMA), to obtain a good BER performance similar to that of MC-CDMA [6]–[8]. The conventional FDE requires the insertion of guard interval (GI) to avoid the inter-block interference (IBI); however, the GI insertion reduces the transmission efficiency. Recently, an FDE technique that requires no GI insertion, called the overlap FDE, was proposed for the single-carrier transmission [9], [10]. The overlap FDE can also be applied to MC-CDMA. In this paper, we apply overlap FDE to MC-CDMA downlink transmission and present the theoretical BER analysis of MC-CDMA with overlap FDE.

The remainder of this paper is organized as follows. Section 2 describes overlap FDE. The transmission system model of MC-CDMA using the overlap FDE is presented in Sect. 3. The conditional BER analysis is presented in Sect. 4. In Sect. 5, the theoretical average BER in a frequency-selective Rayleigh fading channel is numerically evaluated by Monte-Carlo numerical computation method using the derived conditional BER and is confirmed by computer simulation of the signal transmission. Section 6 offers some conclusions.

## 2. Overlap FDE

For the conventional FDE, the GI is inserted so that the received signal block over the fast Fourier transform (FFT) block becomes a circular convolution between the channel impulse response and the transmitted signal block. Without the GI insertion, the inter-block interference (IBI) is present only around the beginning of the received signal block. The residual IBI after the MMSE-FDE is given by the circular convolution between the IBI and the MMSE-FDE filter impulse response. The impulse response of MMSE-FDE filter is shown in Fig. 1 for an FFT block size of 512 samples and a sample-spaced $L$ = 16-path Rayleigh fading channel with uniform power delay profile. As seen from Fig. 1, the impulse response concentrates at the vicinity of $t = 0$. Therefore, the residual IBI after MMSE-FDE is localized near the both ends of FFT block. This is exploited by the overlap

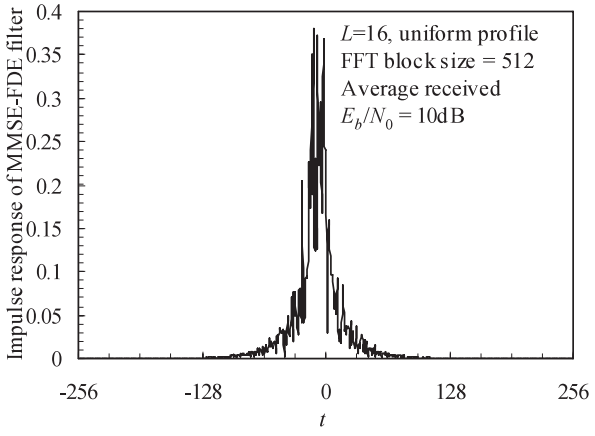


**Fig. 1** Impulse response of MMSE-FDE filter.

Manuscript received August 30, 2006.
Manuscript revised May 2, 2007.

[†]The authors are with the Dept. of Electrical and Communication Engineering, Graduate School of Engineering, Tohoku University, Sendai-shi, 980-8579 Japan.
a) E-mail: tomeba@mobile.ecei.tohoku.ac.jp

DOI: 10.1093/ietcom/e91–b.3.795

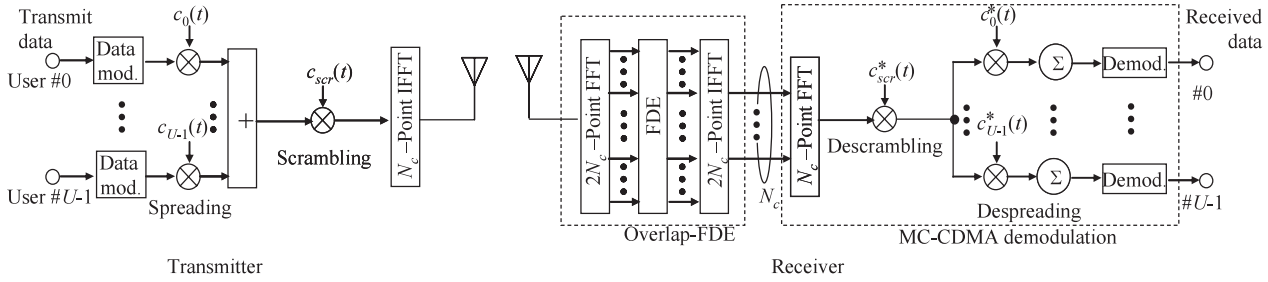


**Fig. 3** Transmitter/receiver structure for MC-CDMA downlink.

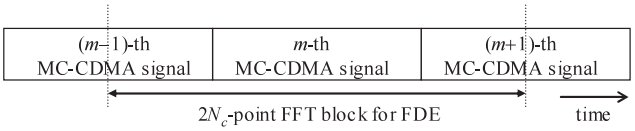


**Fig. 2** Overlap FDE for the reception of the $m$-th MC-CDMA signal.

FDE to suppress the IBI. For performing overlap FDE, the FFT block size is increased to an integral multiple of $N_c$, as shown in Fig. 2. A central part of $N_c$ samples is picked up from the equalized output. By doing so, the residual IBI can be sufficiently suppressed. By increasing the FFT block size, the residual IBI can be suppressed more; however, the computational complexity increases. In this paper, we assume an FFT block size of $2N_c$ samples.

## 3. Transmission System Model

In this paper, the downlink transmission is considered. Figure 3 illustrates the transmitter and receiver structure for MC-CDMA with overlap FDE. Throughout the paper, sample-spaced discrete-time signal representation is used.

At the transmitter, $U$ data symbol sequences $d_u(i)$, $u = 0 \sim (U-1)$, to be transmitted are respectively spread by orthogonal spreading codes $\{c_u(t);\ t = 0 \sim (SF-1)\}$, $u = 0 \sim (U-1)$, to obtain the multi-code chip sequence, where $SF$ denotes the spreading factor, and further multiplied with a scrambling sequence $c_{scr}(t)$. To generate the MC-CDMA signal with $N_c$ subcarriers, $N_c$-point IFFT is applied. In the conventional MC-CDMA transmitter, the guard interval (GI) is inserted to the transmit signal. However, overlap FDE requires no GI insertion, thereby, the transmission efficiency is improved.

At the receiver, $2N_c$-point FFT is applied to decompose the received signal into $2N_c$ frequency components, and the FDE is applied. The time-domain signal of $2N_c$ samples is recovered by $2N_c$-point IFFT. After picking up the $N_c$-sample center part, MC-CDMA signal demodulation is carried out.

### 3.1 Transmit Signal

The MC-CDMA signal $s(t)$ can be expressed using the equivalent low-pass representation as

$$s(t) = \sum_{m=-\infty}^{\infty} s_m(t - mN_c), \tag{1}$$

where

$$s_m(t) = \begin{cases} \displaystyle\sum_{k=0}^{N_c-1} S_m(k) \exp\left(j2\pi k \frac{t}{N_c}\right), & t = 0 \sim (N_c - 1) \\ 0, & \text{otherwise} \end{cases} \tag{2}$$

is the $m$-th MC-CDMA signal, and $S_m(k)$ is the $k$-th ($k = 0 \sim (N_c - 1)$) subcarrier component of the $m$-th MC-CDMA signal, given as

$$S_m(k) = \sqrt{\frac{2P}{SF}} \sum_{u=0}^{U-1} c_{scr}(k) c_u(k \bmod SF) d_u \cdot \left(\lfloor k/SF \rfloor + m\frac{N_c}{SF}\right). \tag{3}$$

In Eq. (3), $P$ is the transmit power per user and $\lfloor x \rfloor$ is the largest integer smaller than or equal to $x$.

### 3.2 Received Signal

The MC-CDMA signal $s(t)$ is transmitted over a frequency-selective fading channel. We assume a sample-spaced $L$-path frequency-selective block fading channel. The complex-valued path gain and time delay of the $l$-th propagation path are denoted by $h_l$ and $\tau_l$, respectively. We assume $\tau_l = lT_c$, where $T_c$ is the FFT/IFFT sampling period. The received signal $r(t)$ is expressed as

$$r(t) = \sum_{l=0}^{L-1} h_l s(t - l). \tag{4}$$

$2N_c$-point FFT is applied to decompose the received signal block $\{r(t);\ t = (m - 1/2)N_c \sim ((m + 3/2)N_c - 1)\}$ into $2N_c$ frequency components for the reception of the $m$-th MC-CDMA signal as shown in Fig. 4. For performing FFT, the desired signal block needs to be expressed as a circular convolution between the channel impulse response and the transmitted signal block of $2N_c$ samples. Since the GI is not inserted, the IBI appears. We express $r(t)$ for $t = (m-1/2)N_c \sim ((m+3/2)N_c-1)$ by using $r_m(t)$ as $r(t) = r_m(t-(m-1/2)N_c)$. $r_m(t)$ is given as

$$r_m(t) = \sum_{l=0}^{L-1} h_l y_m((t - l) \bmod 2N_c) + \nu_m(t) + \eta_m(t) \tag{5}$$

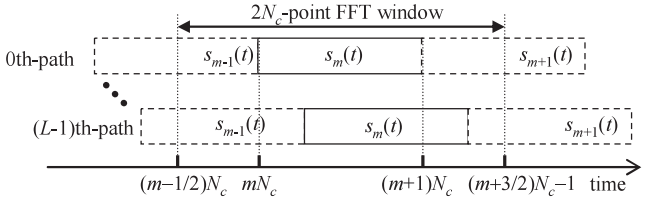


**Fig. 4** Received signal.

for $t = 0 \sim (2N_c - 1)$, where $y_m(t)$ is the transmitted signal block of $2N_c$ samples, $\nu_m(t)$ is the IBI, and $\eta_m(t)$ is the additive white Gaussian noise (AWGN) with zero mean and variance $2N_0/T_c$ with $N_0$ being the single-sided power spectrum density. $y_m(t)$ and $\nu_m(t)$ are given as

$$y_m(t) = \begin{cases} s_{m-1}\left(t + \dfrac{1}{2}N_c\right), & t = 0 \sim \dfrac{1}{2}N_c - 1 \\ s_m\left(t - \dfrac{1}{2}N_c\right), & t = \dfrac{1}{2}N_c \sim \dfrac{3}{2}N_c - 1 \\ s_{m+1}\left(t - \dfrac{3}{2}N_c\right), & t = \dfrac{3}{2}N_c \sim 2N_c - 1 \end{cases}, \quad (6)$$

$$\begin{aligned} \nu_m(t) = \sum_{l=0}^{L-1} h_l \{ & y_{m-2}((t-l) \bmod 2N_c) \\ & - y_m((t-l) \bmod 2N_c)\} \times \{u_0(t) - u_0(t-l)\}, \end{aligned} \quad (7)$$

where $u_0(t)$ is the unit step function.

### 3.3 Overlap FDE

$2N_c$-point FFT is applied to decompose the received signal $r_m(t)$ into $2N_c$ frequency components $\{R_m(q); q = 0 \sim (2N_c - 1)\}$. $R_m(q)$ is given as

$$\begin{aligned} R_m(q) &= \frac{1}{2N_c} \sum_{t=0}^{2N_c-1} r_m(t) \exp\left(-j2\pi q \frac{t}{2N_c}\right) \\ &= H(q)Y_m(q) + N_m(q) + \Pi_m(q), \end{aligned} \quad (8)$$

where

$$\begin{cases} H(q) = \displaystyle\sum_{l=0}^{L-1} h_l \exp\left(-j2\pi q \frac{l}{2N_c}\right) \\ Y_m(q) = \dfrac{1}{2N_c} \displaystyle\sum_{t=0}^{2N_c-1} y_m(t) \exp\left(-j2\pi q \frac{t}{2N_c}\right) \\ N_m(q) = \dfrac{1}{2N_c} \displaystyle\sum_{t=0}^{2N_c-1} \nu_m(t) \exp\left(-j2\pi q \frac{t}{2N_c}\right) \\ \Pi_m(q) = \dfrac{1}{2N_c} \displaystyle\sum_{t=0}^{2N_c-1} \eta_m(t) \exp\left(-j2\pi q \frac{t}{2N_c}\right) \end{cases}. \quad (9)$$

Then, $R_m(q)$ is multiplied by the FDE weight $w(q)$ as

$$\hat{R}_m(q) = R_m(q)w(q) = \hat{H}(q)Y_m(q) + \hat{N}_m(q) + \hat{\Pi}_m(q), \quad (10)$$

where

$$\begin{cases} \hat{H}(q) = H(q)w(q) \\ \hat{N}_m(q) = N_m(q)w(q) \\ \hat{\Pi}_m(q) = \Pi_m(q)w(q) \end{cases}. \quad (11)$$

We consider three FDE weights: zero-forcing (ZF), maximal ratio combining (MRC) and MMSE, given as [4], [5]:

$$w(q) = \begin{cases} \dfrac{H^*(q)}{|H(q)|^2}, & \text{ZF} \\ H^*(q), & \text{MRC} \\ \dfrac{H^*(q)}{\dfrac{U}{SF}|H(q)|^2 + (P/\sigma^2)^{-1}}, & \text{MMSE} \end{cases}, \quad (12)$$

where $2\sigma^2$ is the variance of the IBI plus noise. The ZF weight can perfectly restore the frequency-nonselective channel. The MRC weight maximizes the received signal-to-noise power ratio (SNR). The MMSE weight minimizes the mean square error (MSE) between $Y_m(q)$ and $\hat{R}_m(q)$ as

$$w(q) = \arg\min_{\{w(q)\}} E[|\hat{R}_m(q) - Y_m(q)|^2], \quad (13)$$

where $E[\cdot]$ denotes the expectation operation.

After the FDE, $2N_c$-point IFFT is applied to $\{\hat{R}_m(q); q = 0 \sim (2N_c - 1)\}$ to obtain the time-domain signal as

$$\hat{r}_m(t) = \sum_{q=0}^{2N_c-1} \hat{R}_m(q) \exp\left(j2\pi t \frac{q}{2N_c}\right). \quad (14)$$

To suppress the residual IBI, we pick up the center part of $N_c$ samples of $\hat{r}_m(t)$. The resulting output $\hat{s}_m(t)$, $t = 0 \sim (N_c - 1)$, can be expressed as

$$\hat{s}_m(t) = \hat{r}_m(t + N_c/2). \quad (15)$$

MC-CDMA demodulation is done by applying $N_c$-point FFT to $\{\hat{s}_m(t); t = 0 \sim (N_c - 1)\}$ as

$$\begin{aligned} \hat{S}_m(k) &= \frac{1}{N_c} \sum_{t=0}^{N_c-1} \hat{s}_m(t) \exp\left(-j2\pi k \frac{t}{N_c}\right) \\ &= \hat{H}(2k)S_m(k) + X_m(k) + \tilde{N}_m(k) + \tilde{\Pi}_m(k), \end{aligned} \quad (16)$$

where $X_m(k)$, $\tilde{N}_m(k)$, and $\tilde{\Pi}_m(k)$ are the residual inter-symbol interference (ISI) from the $(m-1)$-th and $(m+1)$-th MC-CDMA symbols, the residual IBI, and noise, respectively. They are expressed as

$$\begin{cases} X_m(k) = \dfrac{1}{N_c} \displaystyle\sum_{\tau=N_c/2}^{N_c-1} \{s_{m-1}(\tau) - s_m(\tau)\}\phi(k,\tau) \\ \qquad + \dfrac{1}{N_c} \displaystyle\sum_{\tau=0}^{N_c/2-1} \{s_{m+1}(\tau) - s_m(\tau)\}\phi(k,\tau) \\ \tilde{N}_m(k) = \dfrac{1}{N_c} \displaystyle\sum_{l=0}^{L-1} h_l \sum_{\tau=0}^{l-1} \{s_{m-1}(N_c/2 + \tau - l) \\ \qquad - s_{m+1}(N_c/2 + \tau - l)\}\psi(k,\tau) \\ \tilde{\Pi}_m(k) = \dfrac{1}{N_c} \displaystyle\sum_{\tau=0}^{2N_c-1} \eta_m(\tau)\psi(k,\tau) \end{cases}, \quad (17)$$

where

$$\begin{cases} \phi(k,\tau) = \displaystyle\sum_{t=0}^{N_c-1} \hat{h}\,(t+N_c-\tau)\exp\left(-j2\pi k\frac{t}{N_c}\right) \\ \psi(k,\tau) = \displaystyle\sum_{t=0}^{N_c-1} \omega\left(t+\frac{1}{2}N_c-\tau\right)\exp\left(-j2\pi k\frac{t}{N_c}\right) \end{cases} \tag{18}$$

with

$$\begin{cases} \hat{h}(\tau) = \displaystyle\sum_{q=0}^{2N_c-1} \hat{H}(q)\exp\left(j2\pi\tau\frac{q}{2N_c}\right) \\ \omega(\tau) = \displaystyle\sum_{q=0}^{2N_c-1} w(q)\exp\left(j2\pi\tau\frac{q}{2N_c}\right) \end{cases}. \tag{19}$$

After the descrambling and despreading, the decision variable $\hat{d}_u(i)$ corresponding to $d_u(i)$ is obtained as

$$\begin{aligned} \hat{d}_u(i) &= \frac{1}{SF}\sum_{k=iSF}^{(i+1)SF-1} \hat{S}_m(k)c^*_{scr}(k)c^*_u(k \bmod SF) \\ &= \sqrt{\frac{2P}{SF}}\left(\frac{1}{SF}\sum_{k=iSF}^{(i+1)SF-1}\hat{H}(2k)\right)d_u(i) \\ &\quad + \hat{\Lambda}_u + \hat{X}_u + \hat{N}_u + \hat{\Pi}_u, \end{aligned} \tag{20}$$

where $\hat{\Lambda}_u$ denotes the residual inter-code interference (ICI) and

$$\begin{cases} \hat{\Lambda}_u = \dfrac{1}{SF}\sqrt{\dfrac{2P}{SF}}\displaystyle\sum_{\substack{u'=0\\ \neq u}}^{U-1} d_u(i)\left(\sum_{k=iSF}^{(i+1)SF-1}\hat{H}(2k)c_{u'}(k)c^*_u(k)\right) \\ \hat{X}_u = \dfrac{1}{SF}\displaystyle\sum_{k=iSF}^{(i+1)SF-1} X_m(k)c^*_{scr}(k)c^*_u(k) \\ \hat{N}_u = \dfrac{1}{SF}\displaystyle\sum_{k=iSF}^{(i+1)SF-1} \tilde{N}_m(k)c^*_{scr}(k)c^*_u(k) \\ \hat{\Pi}_u = \dfrac{1}{SF}\displaystyle\sum_{k=iSF}^{(i+1)SF-1} \tilde{\Pi}_m(k)c^*_{scr}(k)c^*_u(k) \end{cases}. \tag{21}$$

## 4. BER Analysis

We assume the quaternary phase shift keying (QPSK) data modulation and all '1' data transmission. A conditional BER expression for MC-CDMA with overlap FDE in a frequency-selective Rayleigh fading channel is derived. Without loss of generality, $d_0(0)$ is to be detected.

From Eq. (20), the decision variable $\hat{d}_0(0)$ is given by

$$\begin{aligned} \hat{d}_0(0) &= \sqrt{\frac{2P}{SF}}\left(\frac{1}{SF}\sum_{k=0}^{SF-1}\hat{H}(2k)\right)d_0(0) \\ &\quad + \hat{\Lambda}_0 + \hat{X}_0 + \hat{N}_0 + \hat{\Pi}_0. \end{aligned} \tag{22}$$

It can be understood from Eq. (22) that $\hat{d}_0(0)$ is a complex-valued random variable with mean $\sqrt{2P/SF}((1/SF)\sum_{k=0}^{SF-1}\hat{H}(2k))d_0(0)$. Approximating $\hat{\Lambda}_0$, $\hat{X}_0$, and $\hat{N}_0$as a zero-mean complex-valued Gaussian variable, $\mu = \hat{\Lambda}_0 + \hat{X}_0 + \hat{N}_0 + \hat{\Pi}_0$ can be treated as a new zero-mean complex-valued Gaussian variable. The variance $2\sigma^2_\mu$ of $\mu$ is given by

$$2\sigma^2_\mu = 2\sigma^2_\Lambda + 2\sigma^2_X + 2\sigma^2_N + 2\sigma^2_\Pi. \tag{23}$$

From Eq. (21), $\sigma^2_\Lambda$, $\sigma^2_X$, $\sigma^2_N$ and $\sigma^2_\Pi$ can be derived as (see Appendix)

$$\begin{cases} \sigma^2_\Lambda = E[|\hat{\Lambda}_0|^2]/2 \\ \quad = P\dfrac{U-1}{SF^2}\left(\dfrac{1}{SF}\displaystyle\sum_{k=0}^{SF-1}|\hat{H}(2k)|^2 - \left|\dfrac{1}{SF}\sum_{k=0}^{SF-1}\hat{H}(2k)\right|^2\right) \\ \sigma^2_X = E[|\hat{X}_0|^2]/2 = 2P\dfrac{U}{SF^3}\dfrac{1}{N_c}\displaystyle\sum_{\tau=0}^{N_c-1}\sum_{k=0}^{SF-1}|\phi(k,\tau)|^2 \\ \sigma^2_N = E[|\hat{N}_0|^2]/2 \\ \quad = 2P\dfrac{U}{SF^3}\dfrac{1}{N_c}\displaystyle\sum_{l=0}^{L-1}|h_l|^2\left(\sum_{\tau=0}^{l-1}\sum_{k=0}^{SF-1}|\psi(k,\tau)|^2\right) \\ \sigma^2_\Pi = E[|\hat{\Pi}_0|^2]/2 \\ \quad = \dfrac{1}{SF^2}\dfrac{N_0}{N_cT_c}\dfrac{1}{N_c}\displaystyle\sum_{\tau=0}^{2N_c-1}\left(\sum_{k=0}^{SF-1}|\psi(k,\tau)|^2\right) \end{cases}. \tag{24}$$

The conditional BER for the given $\boldsymbol{H} = [H(0), H(1), \ldots, H(2N_c-1)]$ can be given by [2]

$$P_b\left(\frac{E_s}{N_0}, \boldsymbol{H}\right) = \frac{1}{2}\mathrm{erfc}\left[\sqrt{\frac{1}{4}\gamma\left(\frac{E_s}{N_0}, \boldsymbol{H}\right)}\right], \tag{25}$$

where $\mathrm{erfc}[x] = (2/\sqrt{\pi})\int_x^\infty \exp(-t^2)dt$ is the complementary error function and $\gamma(E_s/N_0,\ \boldsymbol{H})$ is the conditional signal-to-interference plus noise power ratio (SINR), which is given by

$$\begin{aligned} \gamma\left(\frac{E_s}{N_0}, \boldsymbol{H}\right) &= \frac{\left|\sqrt{\dfrac{2P}{SF}}\left(\dfrac{1}{SF}\displaystyle\sum_{k=0}^{SF-1}\hat{H}(2k)\right)d_0(0)\right|^2}{\sigma^2_\mu} \\ &= \frac{2\dfrac{E_s}{N_0}\left|\dfrac{1}{SF}\displaystyle\sum_{k=0}^{SF-1}\hat{H}(2k)\right|^2}{\left(\dfrac{U-1}{SF}\dfrac{E_s}{N_0}\right)\left(\dfrac{1}{SF}\displaystyle\sum_{k=0}^{SF-1}|\hat{H}(2k)|^2 - \left|\dfrac{1}{SF}\sum_{k=0}^{SF-1}\hat{H}(2k)\right|^2\right)} \\ &\quad + 2\left(\frac{U}{SF}\frac{E_s}{N_0}\right)\frac{1}{N_c}\sum_{\tau=0}^{N_c-1}\frac{1}{SF}\sum_{k=0}^{SF-1}|\phi(k,\tau)|^2 \\ &\quad + 2\left(\frac{U}{SF}\frac{E_s}{N_0}\right)\frac{1}{N_c}\sum_{l=0}^{L-1}|h_l|^2\sum_{\tau=0}^{l-1}\frac{1}{SF}\sum_{k=0}^{SF-1}|\psi(k,\tau)|^2 \\ &\quad + \frac{1}{N_c}\sum_{\tau=0}^{2N_c-1}\frac{1}{SF}\sum_{k=0}^{SF-1}|\psi(k,\tau)|^2, \end{aligned} \tag{26}$$

where $E_s = PN_cT_c$ is the data symbol energy. The average BER can be numerically evaluated by averaging Eq. (25) over all possible $\boldsymbol{H}$:

$$P_b(E_s/N_0) = \underset{all\ \boldsymbol{H}}{\text{average}}[P_b(E_s/N_0, \boldsymbol{H})]. \quad (27)$$

## 5. Numerical and Simulation Results

The numerical and simulation conditions are summarized in Table 1. A sample-spaced $L = 16$-path frequency-selective block Rayleigh fading channel with uniform power delay profile (i.e., the ensemble average of $|h_l|^2$ is $1/L$ for all $l$) and the ideal channel estimation are assumed. For comparison, the BER performance of conventional MC-CDMA transmission with GI insertion of $N_g = 32$ samples is also presented.

### 5.1 Average BER Performance

The impulse response of MMSE-FDE filter is shown in Fig. 1 and those of MRC- and ZF-FDE filters are shown in Fig. 5. Since the impulse response of MRC-FDE filter exists only at the vicinity of $t = 0$ and lasts only $L-1$ samples, the overlap MRC-FDE can perfectly suppress the IBI. However, since MRC enhances the frequency-selectivity of the channel, the residual ICI$\hat{\Lambda}_0$ and residual ISI$\hat{X}_0$ get stronger (note that the ICI is not present at all in the case of OFDM), producing very high BER floor. On the other hand, ZF-FDE can restore the frequency-nonselective channel, the ISI is not produced. However, since the impulse response of ZF-FDE filter spreads over an entire $2N_c$-sample block, the IBI cannot be suppressed. As shown in Fig. 1, although the impulse response of MMSE-FDE filter spreads more than the MRC-FDE filter, it is still concentrated around $t = 0$ and therefore can sufficiently suppress the IBI.

Figure 6 plots the average BER performance of MC-CDMA using overlap FDE as a function of the average received $E_b/N_0$ ($= 0.5(E_s/N_0)$) for the case of QPSK. For comparison, the BER performance of conventional MC-CDMA with GI insertion of $N_g = 32$ is also plotted in Fig. 6, where the $E_b/N_0$ loss due to GI insertion is taken into account.

Figure 6(a) shows the results for $SF$=1 (OFDM). The MMSE weight provides the best BER performance among three weights. Overlap MMSE-FDE gives almost the same BER performance as the conventional MMSE-FDE. However, since overlap FDE cannot perfectly suppress the IBI, error floor is seen in high average received $E_b/N_0$ regions.

Figure 6(b) shows the average BER performance with the overlap-FDE when $SF$=$U$ = 16. Note that the frequency block inter-leaver is used to take advantage of the channel frequency-selectivity and hence to improve the BER performance. The BER performance with the overlap MMSE-FDE can be further improved since larger frequency diversity gain is obtained, and almost the same BER performance is obtained as with the conventional MMSE-FDE. On the other hand, MRC-FDE weight can also obtain the large frequency diversity gain; however, the orthogonality among orthogonal codes is distorted due to enhanced frequency-selectivity and therefore, the large ICI is produced. ZF-FDE provides no ICI; however, since the frequency diversity gain cannot be obtained, the BER performance with ZF-FDE is worse than that with MMSE-FDE. The simulated BERs are also plotted in Fig. 6. A fairly good agreement between the theoretical and simulation results is seen.

Figure 7 plots the simulated BER performance for

**Table 1** Numerical and simulation conditions.

| | | |
|---|---|---|
| Data modulation | | QPSK, 16QAM |
| MC-CDMA | No. of sub-carriers | $N_c$=256 |
| | Scrambling code | 4095-chip PN |
| | Spreading codes | Walsh codes |
| | Spreading factor | $SF$=1, 16 |
| | No. of users | $U$=1, 16 |
| Channel model | No. of paths | $L$=16 |
| | Power delay profile | Uniform |
| | Time delay | $\tau_l$=$l$, $l$=0~$L$−1 |
| Overlap FDE | FFT block size | 512 (=2$N_c$) |
| | FDE weight | MMSE, MRC, ZF |
| Channel estimation | | Ideal |

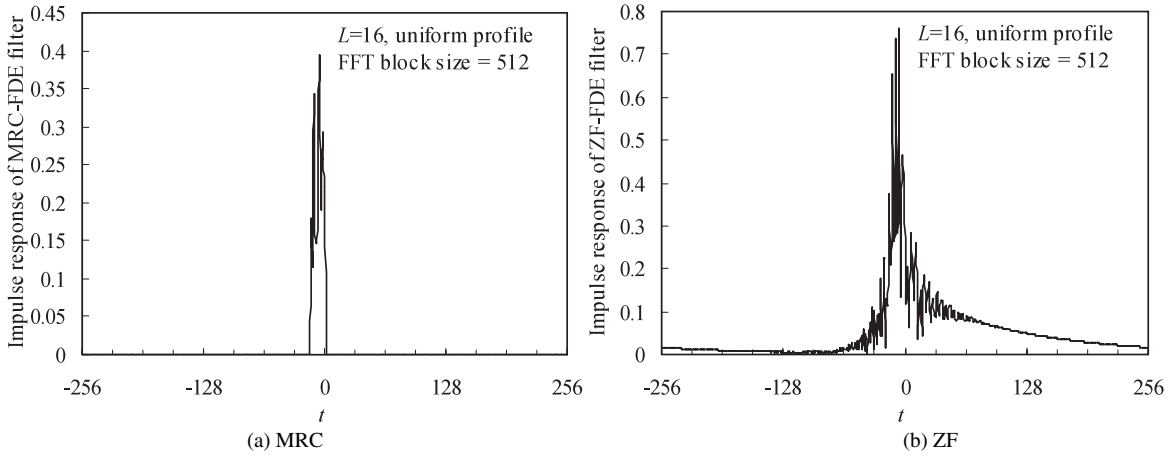


**Fig. 5** Impulse responses of MRC- and ZF-FDE filters.

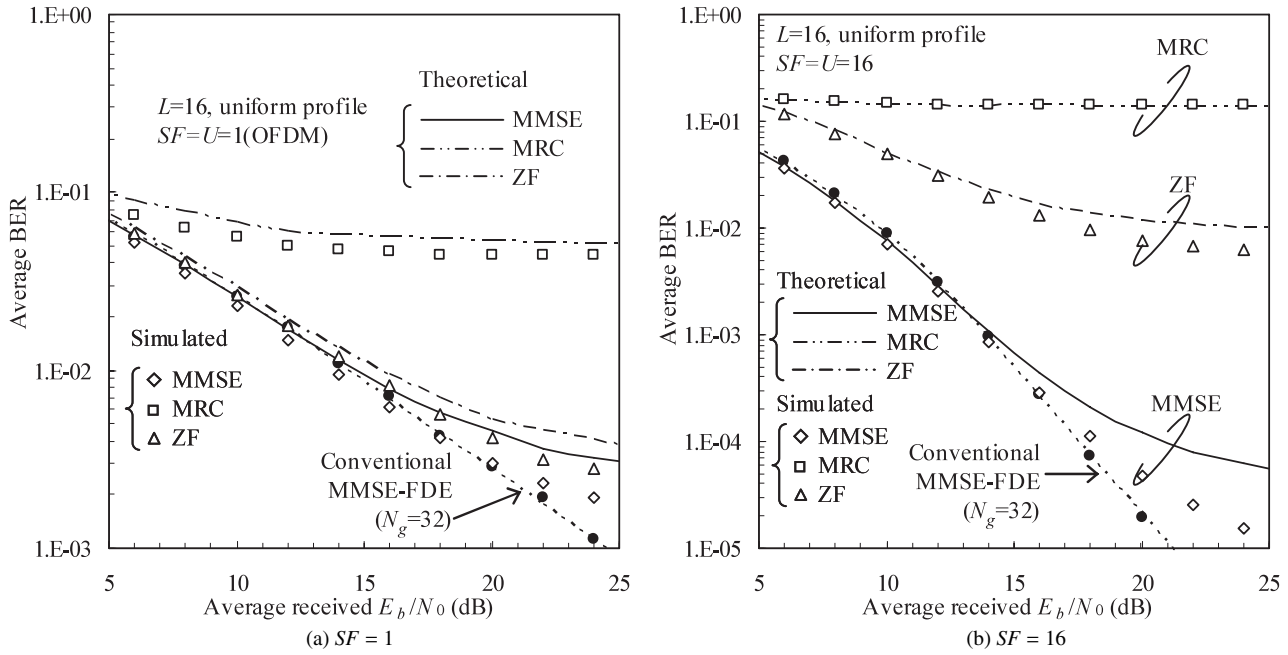


**Fig. 6** Average BER performance. QPSK.

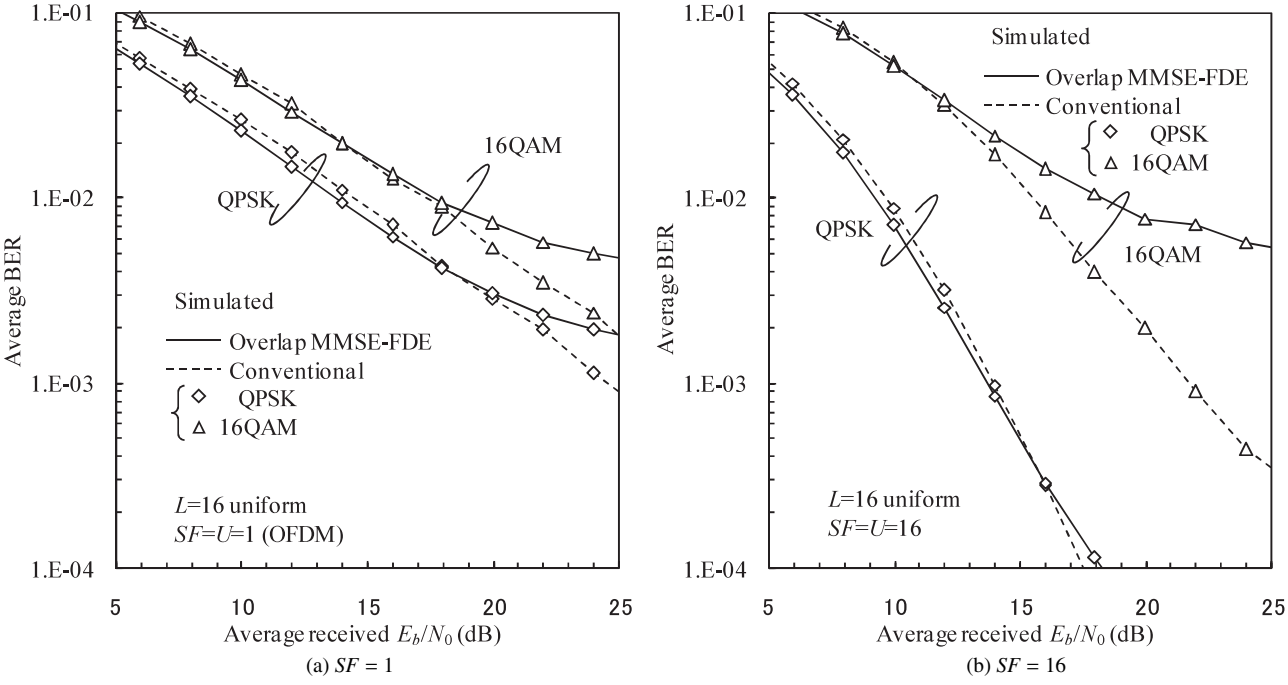


**Fig. 7** Average BER performance. 16QAM.

16QAM. When $SF = 1$ (OFDM), the overlap MMSE-FDE gives worse performance than the conventional FDE, due to the residual IBI in a high average received $E_b/N_0$ region. The performance degradation is larger for 16QAM than QPSK. This is because the Euclidian distance between neighboring symbols is shorter for 16QAM, and therefore, the decision error due to the residual IBI is more likely than for QPSK. On the other hand, when $SF = 16$, high BER floor is seen for the overlap MMSE-FDE when 16QAM is used. This is because the residual ICI is also present in addition to the residual IBI.

### 5.2 Overlap FDE with $N_c$-Point FFT/IFFT

So far, overlap FDE that requires the $2N_c$-point FFT/IFFT was presented. An overlap FDE using $N_c$-point FFT/IFFT can also be used. In this case, the received MC-CDMA signal stream is divided into a sequence of $N_c/2$-sample blocks,

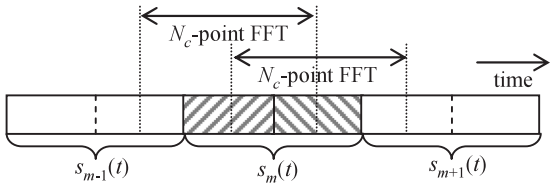


**Fig. 8** Overlap FDE using $N_c$-point FFT/IFFT.

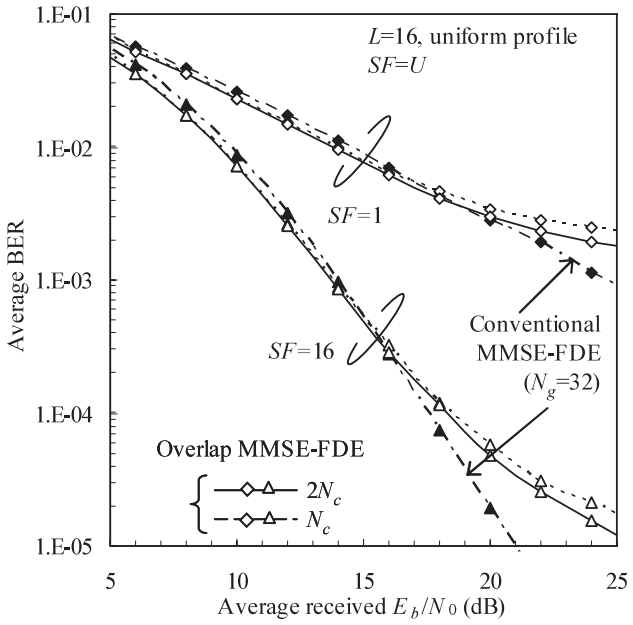


**Fig. 9** Performance comparison of the overlap MMSE-FDE using $N_c$- and $2N_c$-point FFT/IFFT.

**Table 2** Computational complexity of the overlap FDE.

| | Number of complex multiplication operations |
|---|---|
| Overlap FDE using $N_c$-point FFT/IFFT | $2(2(N_c\log_2 N_c))+2N_c$ |
| Overlap FDE using $2N_c$-point FFT/IFFT | $2(2N_c\log_2 2N_c)+2N_c$ |

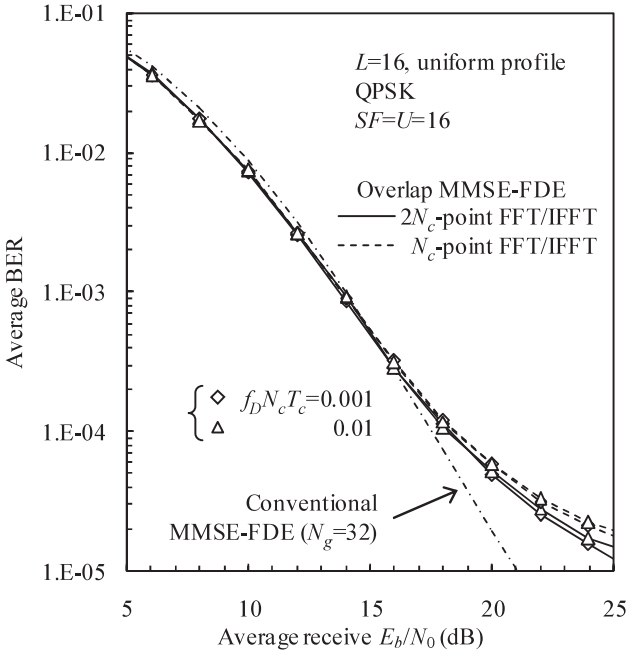


**Fig. 10** Impact of Doppler frequency. $SF$ = 16.

then, $N_c$-point FFT is applied over an $N_c$-sample interval which includes an $N_c/2$-sample signal block of interest in its center as shown in Fig. 8. After FDE, the time-domain $N_c$-sample block is obtained by $N_c$-point IFFT. Only an $N_c/2$-sample center part of $N_c$-samples equalized output is picked up in order to suppress the IBI. The resulting sequence of equalized $N_c/2$-sample signal blocks is an equalized MC-CDMA signal stream.

Figure 9 compares the simulated BER performance with the overlap MMSE-FDE using $N_c$- and $2N_c$-point FFT/IFFT with $SF$ as a parameter. It is seen that the BER performance is almost the same irrespective of FFT block size. We compare the computational complexity of the overlap FDE using $2N_c$-point FFT/IFFT and that using $N_c$-point FFT/IFFT in terms of the number of complex multiplication operations required per one MC-CDMA symbol period. For overlap FDE using $2N_c$-point FFT/IFFT, a pair of $2N_c$-point FFT operation and IFFT operation and $2N_c$ complex multiplication operations are required. On the other hand, the overlap FDE using $N_c$-point FFT/IFFT requires two pairs of $N_c$-point FFT operation and IFFT operation and $2N_c$ complex multiplication operations. The computational complexity comparison is shown in Table 2. The overlap FDE using $2N_c$-point FFT/IFFT is only 1.2 times more complex than that using $N_c$-point FFT/IFFT when $N_c$ = 256.

### 5.3 Impact of Doppler Frequency

So far, we have assumed a block fading channel, where the channel gains stay constant over $2N_c$-point FFT block (two MC-CDMA symbols). However, the real propagation channel is time-selective. To discuss the impact of channel time-selectivity, we evaluate the BER performance by computer simulation, assuming that the channel gains stay constant over an $N_c$-sample period (one MC-CDMA symbol). This block fading assumption is used in Ref. [5]. The BER performance is plotted in Fig. 10 for the normalized maximum Doppler frequency $f_D N_c T_c$ = 0.001 and 0.01. Note that $f_D N_c T_c$ = 0.001 (0.01) corresponds to a terminal moving speed of about 80 (800) km/h for an FFT sampling rate of 100 MHz and 5 GHz carrier frequency. As can be understood from Fig. 10, only a slight performance degradation is seen even if overlap FDE using $2N_c$-point FFT/IFFT is used. This indicates that overlap FDE using $2N_c$-point FFT/IFFT is robust against the channel time-selectivity in a practical fading environment.

## 6. Conclusion

In this paper, we applied the overlap FDE that requires no GI insertion to MC-CDMA with $N_c$ subcarriers. For performing overlap FDE, the FFT block size is extended to the integer multiple of $N_c$ for the reception of MC-CDMA signals to suppress the inter-block interference (IBI). With overlap FDE, the transmission efficiency is not reduced at all unlike the conventional FDE. The average BER analysis of the overlap FDE was presented, and was confirmed by the computer simulation assuming a frequency-selective Rayleigh fading channel. It was shown that the overlap MMSE-FDE can provide almost the same BER performance as the conventional MMSE-FDE using GI insertion for the case of QPSK. However, in the case of 16QAM, the BER performance of overlap MMSE-FDE significantly degrades due to the presence of residual inter-code interference (ICI) and residual IBI. An ICI cancellation technique [12] can be used to improve the BER performance. Applying ICI cancellation to overlap FDE is left as an interesting future study topic. In this paper, we assumed ideal channel estimation. However, in the practical system, the channel must be estimated. Channel estimation without GI insertion is also an interesting future study.

### References

[1] W.C. Jakes, Jr., ed., Microwave mobile communications, Wiley, New York, 1974.
[2] J.G. Proakis, Digital communications, 2nd ed., McGraw-Hill, 1995.
[3] S. Hara and R. Prasad, "Overview of multicarrier CDM," IEEE Commun. Mag., vol.35, no.12, pp.126–133, Dec. 1997.
[4] S. Hara and R. Prasad, "Design and performance of multicarrier CDMA system in frequency-selective Rayleigh fading channels," IEEE Trans. Veh. Technol., vol.48, no.5, pp.1584–1595, Sept. 1999.
[5] T. Sao and F. Adachi, "Comparative study of various frequency equalization techniques for downlink of a wireless OFDM-CDMA systems," IEICE Trans. Commun., vol.E86-B, no.1, pp.352–364, Jan. 2003.
[6] D. Falconer, S.L. Ariyavisitakul, A. Benyamin-Seeyar, and B. Eidson, "Frequency domain equalization for single-carrier broadband wireless systems," IEEE Commun. Mag., vol.40, no.4, pp.58–66, April 2002.
[7] M.V. Clark, "Adaptive frequency-domain equalization and diversity combining for broadband wireless communications," IEEE J. Sel. Areas Commun., vol.16, no.8, pp.1385–1395, Oct. 1998.
[8] F. Adachi, D. Garg, S. Takaoka, and K. Takeda, "Broadband CDMA techniques," IEEE Wireless Commun., vol.12, no.2, pp.8–18, April 2005.
[9] I. Martoyo, T. Weiss, F. Capar, and F.K. Jondral, "Low complexity CDMA downlink receiver based on frequency domain equalization," IEEE Vehicular Technology Conference (VTC)'03 Fall, Orlando, Florida, USA, Sept. 2003.
[10] C.V. Sinn and J. Gotze, "Avoidance of guard periods in block transmission systems," 4-th IEEE Workshop on Signal Processing Advances in Wireless Communications (SPAWC)'03, pp.432–436, Rome, Italy, June 2003.
[11] M.H. Degroot, Probability and statistics, 2nd ed., Addison Wesley, 1986.
[12] K. Ishihara, K. Takeda, and F. Adachi, "Iterative frequency-domain soft interference cancellation for multicode DS- and MC-CDMA transmissions and performance comparison," IEICE Trans. Commun., vol.E89-B, no.12, pp.3344–3355, Dec. 2006.

## Appendix: Variances of Interference and Noise

### A. Inter-Code Interference (ICI)

The frequency-component of desired signal component (the first term of Eq. (22)) before the descrambling and despreading can be expressed as

$$\tilde{S}_m(k) = \sqrt{\frac{2P}{SF}} \left( \frac{1}{SF} \sum_{k=0}^{SF-1} \hat{H}(2k) \right) c_{scr}(k) c_0(k) d_0(0). \quad (\mathrm{A}\cdot 1)$$

Therefore, the residual ICI $\hat{\Lambda}_0$ can be expressed as [12]

$$\hat{\Lambda}_0 = \frac{1}{SF} \sum_{k=0}^{SF-1} (\hat{H}(2k) S_m(k) - \tilde{S}_m(k)) c_0^*(k) c_{scr}^*(k), \quad (\mathrm{A}\cdot 2)$$

which can be rewritten as

$$\begin{aligned} \hat{\Lambda}_0 \;=\; & \sqrt{\frac{2P}{SF^3}} \sum_{k=0}^{SF-1} \left( (\hat{H}(2k) - \bar{H}) \sum_{u=1}^{U-1} c_u(k) d_u(0) c_0^*(k) \right) \\ & + \sqrt{\frac{2P}{SF^3}} d_0(0) \sum_{k=0}^{SF-1} (\hat{H}(2k) - \bar{H}), \end{aligned} \quad (\mathrm{A}\cdot 3)$$

where

$$\bar{H} = (1/SF) \sum_{k=0}^{SF-1} \hat{H}(2k). \quad (\mathrm{A}\cdot 4)$$

Finally, we have

$$\hat{\Lambda}_0 = \frac{1}{SF} \sqrt{\frac{2P}{SF}} \sum_{k=0}^{SF-1} \left( \sum_{u=0}^{U-1} (\hat{H}(2k) - \bar{H}) c_u(k) d_u(0) \right) c_0^*(k). \quad (\mathrm{A}\cdot 5)$$

Using Eq. (A·5) and $E[d_u(0) d_{u'}^*(0)] = \delta(u - u')$, the variance $2\sigma_\Lambda^2$ of the ICI is given by

$$\begin{aligned} 2\sigma_\Lambda^2 \;=\; & E[|\hat{\Lambda}_0|^2] = \frac{1}{SF^2} \frac{2P}{SF} \sum_{u=1}^{U-1} \sum_{k=0}^{SF-1} \left| \hat{H}(2k) - \bar{H} \right|^2 \\ & + \frac{1}{SF^2} \frac{2P}{SF} \sum_{k=0}^{SF-1} \sum_{\substack{k'=0 \\ \neq k}}^{SF-1} (\hat{H}(2k) - \bar{H})(\hat{H}^*(2k') - \bar{H}^*) \\ & \times \sum_{u=1}^{U-1} c_u(k) c_u^*(k') c_0^*(k) c_0(k'). \end{aligned} \quad (\mathrm{A}\cdot 6)$$

The second term of Eq. (A·6) is the sum of $(SF \times (SF - 1) \times (U - 1))$ random variable $\{c_u(k) c_u^*(k') c_0^*(k) c_0(k'); k = 0 \sim (SF - 1)$ and $k' (\neq k) = 0 \sim (SF - 1)\}$ with zero-mean and unit variance. For large $SF$ and $U$, the second term of Eq. (A·6) approaches zero from the law of large numbers [11]. Therefore, $2\sigma_\Lambda^2$ is given as

$$2\sigma_\Lambda^2 = \frac{2P}{SF} \frac{U-1}{SF} \left( \frac{1}{SF} \sum_{k=0}^{SF-1} |\hat{H}(2k)|^2 - \left| \frac{1}{SF} \sum_{k=0}^{SF-1} \hat{H}(2k) \right|^2 \right). \quad (\mathrm{A}\cdot 7)$$

### B. Inter-Symbol Interference (ISI)

Using Eq. (21), the variance $2\sigma_X^2$ of the residual ISI is given as

$$\begin{aligned}2\sigma_X^2 &= E[|\hat{X}_0|^2] \\ &= \frac{1}{SF^2}\frac{1}{N_c^2}\sum_{k=0}^{SF-1}\sum_{k'=0}^{SF-1}\sum_{\tau=N_c/2}^{N_c-1}\sum_{\tau'=N_c/2}^{N_c-1}\phi(k,\tau)\phi^*(k',\tau')c_0^*(k)c_0(k') \\ &\times E\left[\{s_{-1}(\tau)-s_0(\tau)\}\{s_{-1}(\tau')-s_0(\tau')\}^* c_{scr}^*(k)c_{scr}(k')\right] \\ &+\frac{1}{SF^2}\frac{1}{N_c^2}\sum_{k=0}^{SF-1}\sum_{k'=0}^{SF-1}\sum_{\tau=0}^{N_c/2-1}\sum_{\tau'=0}^{N_c/2-1}\phi(k,\tau)\phi^*(k',\tau')c_0^*(k)c_0(k') \\ &\times E\left[\{s_1(\tau)-s_0(\tau)\}\{s_1(\tau')-s_0(\tau')\}^* c_{scr}^*(k)c_{scr}(k')\right]. \quad (A\cdot 8)\end{aligned}$$

Assuming a random scrambling sequence $c_{scr}(k)$ , we have

$$\begin{aligned}&E\left[s_m(\tau)s_m'^*(\tau')c_{scr}^*(k)c_{scr}(k')\right] \\ &\quad = N_c(2PU/SF)\delta(m-m')\delta(\tau-\tau')\delta(k-k'), \quad (A\cdot 9)\end{aligned}$$

and thereby, $2\sigma_X^2$ is given as

$$2\sigma_X^2 = 4P\frac{U}{SF^3}\frac{1}{N_c}\sum_{\tau=0}^{N_c-1}\sum_{k=0}^{SF-1}|\phi(k,\tau)|^2. \quad (A\cdot 10)$$

### C. Inter-Block Interference (IBI)

Using Eq. (21), the variance $2\sigma_N^2$ of the residual IBI is given by

$$\begin{aligned}2\sigma_N^2 &= E[|\hat{N}_0|^2] = \frac{1}{SF^2}\frac{1}{N_c^2}\sum_{k=0}^{SF-1}\sum_{k'=0}^{SF-1}\sum_{l=0}^{L-1}\sum_{l'=0}^{L-1}h_l h_{l'}^* \\ &\times\sum_{\tau=0}^{l-1}\sum_{\tau'=0}^{l-1}\psi(k,\tau)\psi^*(k',\tau')c_0^*(k)c_0(k') \\ &\times E[\{s_{-1}(N_c/2+\tau-l)-s_1(N_c/2+\tau-l)\} \\ &\times\{s_{-1}(N_c/2+\tau'-l')-s_1(N_c/2+\tau'-l')\}^* \\ &\times c_{scr}^*(k)c_{scr}(k')]. \quad (A\cdot 11)\end{aligned}$$

From Eq. (A· 9), Eq. (A· 11) can be rewritten as

$$\begin{aligned}2\sigma_N^2 &= \frac{1}{SF^3}\frac{4PU}{N_c}\sum_{k=0}^{SF-1}\sum_{l=0}^{L-1}|h_l|^2\sum_{\tau=0}^{l-1}|\psi(k,\tau)|^2 \\ &+\frac{1}{SF^3}\frac{4PU}{N_c}\sum_{k=0}^{SF-1}\sum_{l=0}^{L-1}\sum_{\substack{l'=0\\ \neq l}}^{L-1}h_l h_{l'}^*\sum_{\tau=0}^{l-1}\sum_{\substack{\tau'=0\\ \neq\tau}}^{l-1}\psi(k,\tau)\psi^*(k,\tau'). \quad (A\cdot 12)\end{aligned}$$

For large $SF$, the second term of Eq. (A· 12) approaches zero due to the law of large numbers. Therefore, $2\sigma_N^2$ is given as

$$2\sigma_N^2 = 4P\frac{U}{SF^3}\frac{1}{N_c}\sum_{k=0}^{SF-1}\sum_{l=0}^{L-1}|h_l|^2\sum_{\tau=0}^{l-1}|\psi(k,\tau)|^2. \quad (A\cdot 13)$$

### D. Noise

Using Eq. (21), the variance $2\sigma_\Pi^2$ of the noise component is given as

$$\begin{aligned}2\sigma_\Pi^2 &= E[|\hat{\Pi}_0|^2] = \frac{1}{SF^2}\frac{1}{N_c^2} \\ &\times\sum_{k=0}^{SF-1}\sum_{k'=0}^{SF-1}\sum_{\tau=0}^{2N_c-1}\sum_{\tau'=0}^{2N_c-1}\psi(k,\tau)\psi^*(k',\tau')c_0^*(k)c_0(k') \\ &\times E\left[\eta_0(\tau)\eta_0^*(\tau')c_{scr}^*(k)c_{scr}(k')\right], \quad (A\cdot 14)\end{aligned}$$

Since

$$E\left[\eta_m(\tau)\eta_m^*(\tau')c_{scr}^*(k)c_{scr}(k')\right] = \frac{2N_0}{T_c}\delta(\tau-\tau')\delta(k-k') \quad (A\cdot 15)$$

for all $m$, $2\sigma_\Pi^2$ is given as

$$2\sigma_\Pi^2 = \frac{1}{SF^2}\frac{2N_0}{N_cT_c}\frac{1}{N_c}\sum_{\tau=0}^{2N_c-1}\sum_{k=0}^{SF-1}|\psi(k,\tau)|^2. \quad (A\cdot 16)$$

**Hiromichi Tomeba** received his B.S. and M.S. degrees in communications engineering from Tohoku University, Sendai, Japan, in 2004 and 2006. Currently he is a Japan Society for the Promotion of Science (JSPS) research fellow, studying toward his PhD degree at the Department of Electrical and Communications Engineering, Graduate School of Engineering, Tohoku University. His research interests include frequency-domain equalization and antenna diversity techniques for mobile communication systems. He was a recipient of the 2004 and 2005 IEICE RCS (Radio Communication Systems) Active Research Award.

**Kazuaki Takeda** received his B.E., M.S. and Dr.Eng. degrees in communications engineering from Tohoku University, Sendai, Japan, in 2003, 2004 and 2007 respectively. Currently he is a postdoctoral fellow at the Department of Electrical and Communications Engineering, Graduate School of Engineering, Tohoku University. Since 2005, he has been a Japan Society for the Promotion of Science (JSPS) research fellow. His research interests include equalization, interference cancellation, transmit/receive diversity, and multiple access techniques. He was a recipient of the 2003 IEICE RCS (Radio Communication Systems) Active Research Award and 2004 Inose Scientific Encouragement Prize.

**Fumiyuki Adachi** received the B.S. and Dr.Eng. degrees in electrical engineering from Tohoku University, Sendai, Japan, in 1973 and 1984, respectively. In April 1973, he joined the Electrical Communications Laboratories of Nippon Telegraph & Telephone Corporation (now NTT) and conducted various types of research related to digital cellular mobile communications. From July 1992 to December 1999, he was with NTT Mobile Communications Network, Inc. (now NTT DoCoMo, Inc.), where he led a research group on wideband/broadband CDMA wireless access for IMT-2000 and beyond. Since January 2000, he has been with Tohoku University, Sendai, Japan, where he is a Professor of Electrical and Communication Engineering at the Graduate School of Engineering. His research interests are in CDMA wireless access techniques, equalization, transmit/receive antenna diversity, MIMO, adaptive transmission, and channel coding, with particular application to broadband wireless communications systems. From October 1984 to September 1985, he was a United Kingdom SERC Visiting Research Fellow in the Department of Electrical Engineering and Electronics at Liverpool University. He was a co-recipient of the IEICE Transactions best paper of the year award 1996 and again 1998 and, also a recipient of Achievement award 2003. He is an IEEE Fellow and was a co-recipient of the IEEE Vehicular Technology Transactions best paper of the year award 1980 and again 1990 and also a recipient of Avant Garde award 2000. He was a recipient of Thomson Scientific Research Front Award 2004.